Sensing and Bio-Sensing Research 10 (2016) 15–19

Contents lists available at ScienceDirect

Sensing and Bio-Sensing Research

journal homepage: www.elsevier.com/locate/sbsr

Towards point-of-care detection of polymicrobial infections: Rapid colorimetric response using a portable spectrophotometer

Mohit S. Verma [a,b], Jackson M. Tsuji [a], Brad Hall [c], Paul Z. Chen [a], James Forrest [b,d], Lyndon Jones [a,c], Frank X. Gu [a,b,*]

[a] Department of Chemical Engineering, University of Waterloo, 200 University Avenue W, Waterloo, Ontario N2L 3G1, Canada
[b] Waterloo Institute for Nanotechnology, University of Waterloo, 200 University Avenue W, Waterloo, Ontario N2L 3G1, Canada
[c] Centre for Contact Lens Research, University of Waterloo, 200 University Avenue W, Waterloo, Ontario N2L 3G1, Canada
[d] Department of Physics and Astronomy, University of Waterloo, 200 University Avenue W, Waterloo, Ontario N2L 3G1, Canada

ARTICLE INFO

Article history:
Received 7 March 2016
Received in revised form 22 April 2016
Accepted 4 May 2016

Keywords:
Gold nanoparticles
Chemical nose
Biosensor
Bacteria
Pathogen
Transmission electron microscopy

ABSTRACT

Infectious diseases spread rapidly because current diagnostic methods are slow, expensive, and require technical expertise. Biosensors have recently been used as devices that can be deployed at the point-of-care for rapid and accurate diagnosis. Here, we show that a "chemical nose" biosensor based on gold nanoparticles can be coupled with a portable spectrophotometer to detect monomicrobial and polymicrobial solutions of pathogenic bacteria within 2 min of data collection. The design presented here exploits the rapid kinetics of gold nanoparticle aggregation around bacteria, which leads to a dramatic color change. The "chemical nose" produces unique signals based on the surface characteristics of the bacteria—such as the presence of extracellular polymeric substances, distribution of charged lipids, and localization of proteins—and hence provides a versatile platform for detection. We present a biosensor design that can easily be translated to the point-of-care because of its rapid response and simple output.

1. Introduction

Rapid detection of bacteria is crucial in curbing the spread of infectious diseases and preventing epidemics [1,2]. Current methods for detection of bacteria require considerable sample processing, because they detect either nucleic acids or proteins, which need to be extracted from the bacteria [3–5]. Culture-based methods are sensitive but slow because the growth of bacteria can require 1–5 days [2]. Additionally, most methods require sophisticated instruments and/or extensive technical training [1,2]. Rapid diagnosis of infectious diseases needs to be executed at the point-of-care with limited resources. Colorimetric responses are preferred in biosensors because they can be easily deciphered at the point-of-care [2,6,7]. Recently, portable scanners and smartphones have been used for measuring, analyzing, and reporting colorimetric responses when sensing analytes such as proteins [8,9], viruses [10], and bacteria [11].

Gold nanoparticles are playing an increasingly important role in providing a colorimetric response because their color depends on their aggregation state and their local environment [5,12]. Using gold nanoparticles for detecting pathogens typically requires biomodification with antibodies or aptamers for targeting specific analytes [2,5,6,13]. This "lock-and-key" approach is limited [14] because detecting multiple pathogens in a mixture requires a unique targeting biomolecule for each pathogen. A "chemical nose" approach provides a viable alternative to the conventional methods because the "chemical nose" can be trained for various analytes, including mixtures [14–16]. We have previously demonstrated that a "chemical nose" based on gold nanoparticles [17] can be used for identification of various unique pathogens once the system has been trained [18,19]. The gold nanoparticles aggregate in a unique manner around different species of bacteria due to the interactions of nanoparticles with bacterial extracellular polymeric substances [19], lipopolysaccharides (for Gram-negative species) [20], teichoic acids (for Gram-positive species) [21], and lipid domains formed around proteins [22] or in the presence of cationic molecules [23]. In order to implement this "chemical nose" at the point-of-care, here we have exploited the kinetics of the color change of gold nanoparticles in the presence of bacteria. The rapid color change provides sufficient data within 2 min to detect bacteria in monomicrobial and polymicrobial solutions. The portable spectrophotometer design used here has the potential to be translated easily to point-of-care use with the help of smartphone-based spectrophotometers [9,24].

* Corresponding author at: Department of Chemical Engineering, University of Waterloo, 200 University Avenue W, Waterloo, Ontario N2L 3G1, Canada.
E-mail address: frank.gu@uwaterloo.ca (F.X. Gu).

http://dx.doi.org/10.1016/j.sbsr.2016.05.004

2. Materials and methods

2.1. Materials

Gold (III) chloride hydrate ($HAuCl_4 \cdot xH_2O$), cetyltrimethylammonium bromide (CTAB), sodium borohydride, silver nitrate, hydrochloric acid, nitric acid, sodium hydroxide, and L-ascorbic acid were purchased from Sigma-Aldrich (Oakville, ON, Canada). Trisodium citrate dihydrate was purchased from Thermo Fisher Scientific (Burlington, ON, Canada). Scintillation vials (20 mL), BD trypticase soy agar (TSA) culture plates, BD nutrient broth, sodium chloride (ACS grade), Nalgene sterilization filter units (0.2 μm pore size), and calcium alginate swabs were purchase from VWR (Mississauga, ON, Canada). 400 mesh formvar/carbon coated copper grids were obtained from Canemco Inc. (Gore, QC, Canada). *Pseudomonas aeruginosa* (ATCC 9027), *Staphylococcus aureus* (ATCC 6538), and *Escherichia coli* (ATCC 10798) were purchased from Cedarlane Labs (Burlington, ON, Canada). All procured chemicals were used without further purification. The 20 mL vials used for gold nanoseed synthesis were cleaned using 12 M sodium hydroxide and larger glassware was cleaned using aqua regia as described in published protocol [25].

2.2. Spectrophotometer design

A standard optical extinction arrangement was used in the spectrophotometer design as previously described [26]. Briefly, a tungsten-filament lamp with fiber coupling (Ocean Optics HL-2000, Dunedin, FL, USA) was used as a light source and the light was collimated before passing through the cuvette containing nanoparticle solutions. The exiting light was collected into another fiber and directed to the portable spectrometer (Ocean Optics USB4000, Dunedin, FL, USA). Micro-volume disposable polystyrene cuvettes were used for the samples. The entire experimental setup was enclosed in a container to minimize external light and dust.

2.3. Synthesis of gold nanoparticles "chemical nose"

Gold nanoseeds were first synthesized using a published procedure [17–19,27,28]. Briefly, 60 μL of 0.1 M freshly prepared ice-cold sodium borohydride was added to 20 mL of a gold (III) chloride hydrate (2.4×10^{-4} M) and trisodium citrate dihydrate (10^{-4} M) solution under vigorous stirring. The sample was incubated overnight in the dark in ambient conditions, filtered (0.2 μm) and stored at 4 °C until use. Branched and spherical gold nanoparticles were synthesized by modifying published procedure, where CTAB is used as a negative template [17,18]. The amount of silver nitrate used was increased to get a greater distinction between the morphologies of nanoparticles. Briefly, 210 mL of 7.33 mM CTAB and 1.46 mM CTAB were used for branched and spherical nanoparticles respectively. Gold (III) chloride hydrate (8.97 mL, 11 mM) was added to each CTAB solution, followed by silver nitrate (1.34 mL for branched nanoparticles and 0.67 mL for spherical nanoparticles, 10 mM) under moderate stirring. Then, L-ascorbic acid (1.44 mL, 100 mM) was added dropwise and the solution turned clear. The appropriate volume of gold nanoseed (2.24 mL for branched nanoparticles and 5.60 mL for spherical nanoparticles) was immediately added. The nanoparticles were purified by centrifugation at 10,000 rpm (14,087*g*) for 15 min resuspended in 1 mM CTAB solution. These two gold nanoparticle solutions were mixed (1:1 by volume) to obtain the purple "chemical nose" solution.

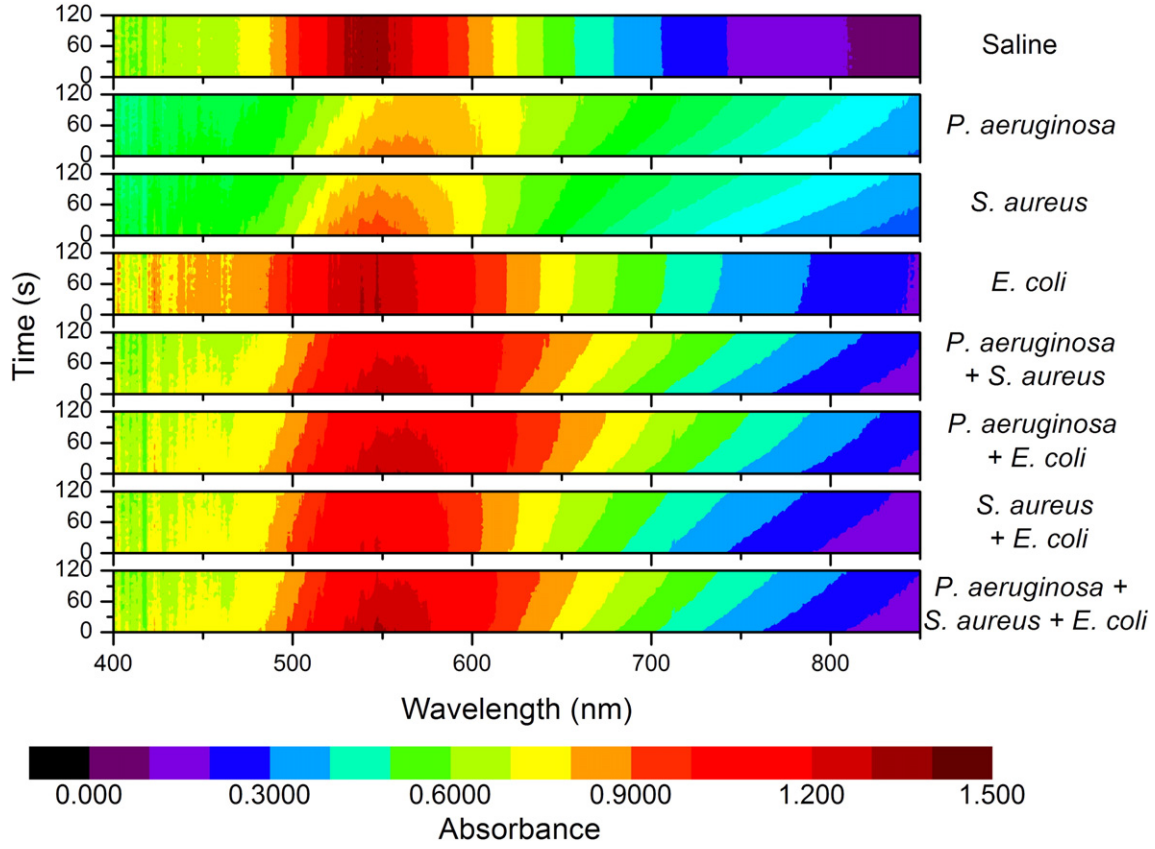

Fig. 1. Changes in absorption spectra of gold nanoparticles over time in the presence of bacteria: saline was used as a control, monomicrobial species were prepared such that the final OD_{660} of bacteria = 0.03 (approximately 5×10^7 CFU/mL), polymicrobial solutions were prepared by mixing 1:1 (v/v) or 1:1:1 (v/v/v) of the monomicrobial solutions. Initial time of zero indicates 1 min after addition of the nanoparticles.

2.4. Bacterial culture

P. aeruginosa, *S. aureus*, and *E. coli* were inoculated on Trypticase Soy Agar (TSA) plates and incubated at 37 °C for 24 h. Bacterial cells were harvested using alginate swabs and suspended in 5 mL of sterile saline (2.55%) with nutrient broth (~0.006%) in a 15 mL centrifuge tube. Each bacterial species was then washed seven times with 2.55% saline (with ~0.006% nutrient broth) by centrifugation at 4000 rpm (3023*g*) for 10 min. The bacteria were then diluted to obtain an optical density at 660 nm (OD_{660}) of 0.10 ± 0.005 (~10^8 CFU/mL [29]). This provides monomicrobial solutions of the bacteria *P. aeruginosa*, *S. aureus* and *E. coli*. Each of these solutions was mixed either 1:1 (v/v) to obtain binary mixtures or 1:1:1 (v/v/v) to obtain a tertiary mixture. The 2.55% saline (with ~0.006%) broth was used as control. This resulted in three monomicrobial and four polymicrobial solutions. When the bacteria are added to gold nanoparticles, the bacterial solution is diluted 1:3 and thus, the final OD_{660} would be 0.03 for bacteria.

2.5. Detection of monomicrobial and polymicrobial solutions

Detection of bacteria was performed in polystyrene cuvettes by mixing 1.2 mL of the "chemical nose" solution and 0.6 mL of the bacterial solution using a pipette (only one replicate was measured per bacterial sample since time-dependent spectra were to be obtained). The cuvette was then transferred to the spectrophotometer and spectra were acquired 60 s after the mixing of nanoparticle and bacteria solutions. The spectra were acquired using Spectra Suite (Ocean Optics, Dunedin, FL, USA) with an integration time of 200 ms, averaging 5 measurements, and with a boxcar width of 5 (boxcar width determines how many adjacent pixels are averaged to report a value for a spectrum; a width of 5 represents that a total of 11 pixels are averaged, 5 on the left and 5 on the right of the pixel being considered). Spectra were obtained every 5 s for 10 min and only the first 2 min of data was used for linear fitting, because it was the linear region of the response. Absorbance values were calculated by using the following formula:

$$\text{Absorbance} = \log_{10}\left(\frac{\text{Intensity}_{\text{sample}}}{\text{Intensity}_{\text{reference}}}\right).$$

Principal component analysis (PCA) was performed using MathWorks® MATLAB® on the absorbance data for 400–850 nm. The first principal component was extracted and fitted using a linear fit for the first 120 s of data.

2.6. Transmission electron microscopy

Polymicrobial mixtures of bacteria with gold nanoparticles (5 μL) were added to formvar-coated copper TEM grids and allowed to dry under ambient conditions overnight. Once dry, the bacteria samples were washed by placing 5 μL of Millipore water on the TEM grids for 30 s and then wicking the liquid using filter paper to remove excess surfactants, salts and unbound gold nanoparticles. The samples were then imaged using Phillips (Eindhoven, The Netherlands) CM10 TEM.

3. Results

3.1. Rapid colorimetric response from portable spectrophotometer

The "chemical nose" we have developed consists of a 1:1 (v/v) mixture of spherical and branched gold nanoparticles. These nanoparticles are cationic because of their CTAB coating. The nanoparticles aggregate around the anionic bacteria and then lead to a rapid and drastic color change. We have demonstrated the potential of this "chemical nose"

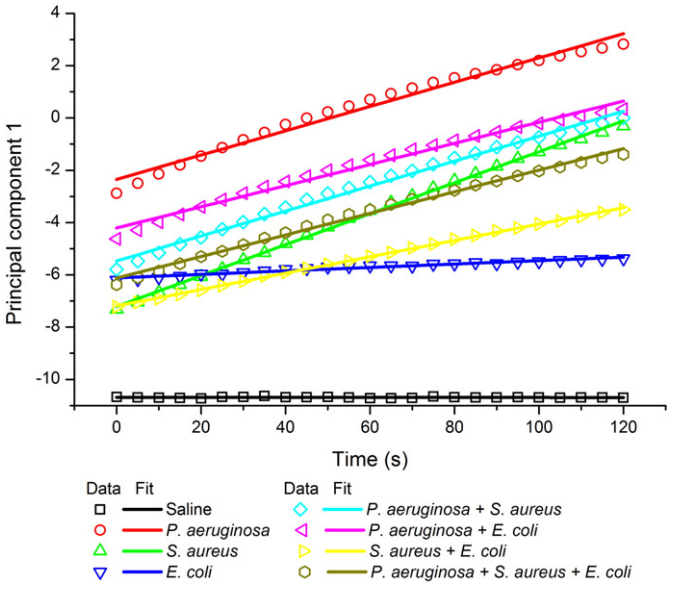

Fig. 2. Linear fit of first principal component (85.1% variance explained) showing unique slopes and intercepts for each monomicrobial and polymicrobial samples.

in differentiating between different species of pathogenic bacteria [18,19,28], but rapid detection of polymicrobial mixtures remained unexplored. With the help of a portable CCD array spectrophotometer, we are translating the "chemical nose" biosensor to point-of-care use. Here, the focus is on a rapid response and a portable device instead of a visual color change, because detection by the naked eye can be challenging to interpret. The CCD spectrophotometer provides a rapid response, hence allowing the study of kinetics of color change in gold nanoparticles. The changes in the spectra over 2 min after mixing bacteria and gold nanoparticles are shown in Fig. 1. Qualitatively, it is observed that saline shows negligible change in the spectra over time, whereas *P. aeruginosa* and *S. aureus* show a drastic change. *E. coli* shows a smaller change compared to the other two bacteria, but a difference can be observed when comparing the response to that of saline. Between *P. aeruginosa* and *S. aureus*, not only is the degree of color change different, but also the rate at which the spectra are changing. These differences are also observed in the responses obtained from binary and tertiary mixtures of these bacteria. It is important to note that the mixtures present a response that can be distinguished from their monomicrobial solutions, which implies that a distinction can be made between monomicrobial and polymicrobial infections.

It can be challenging for the untrained eye to distinguish between some of the contour plots. Thus, the data is simplified using PCA, where the absorbance values of each spectrum are represented by a few principal components. It was determined that the first principal component–whose coefficients for each wavelength are presented in Fig. S1—explained 85.1% of the variance and hence, this component was plotted over time for each of the samples, as shown in Fig. 2. A

Table 1
Slopes and intercepts of linear fits of principal components for each of the bacterial samples.

Sample	Slope	Intercept	R^2
Saline	0.000	−10.685	0.006
Pseudomonas aeruginosa	0.046	−2.349	0.980
Staphylococcus aureus	0.059	−7.211	0.998
Escherichia coli	0.007	−6.112	0.959
P. aeruginosa + *S. aureus*	0.048	−5.468	0.992
P. aeruginosa + *E. coli*	0.040	−4.206	0.986
S. aureus + *E. coli*	0.031	−7.186	0.999
P. aeruginosa + *S. aureus* + *E. coli*	0.041	−6.124	0.993

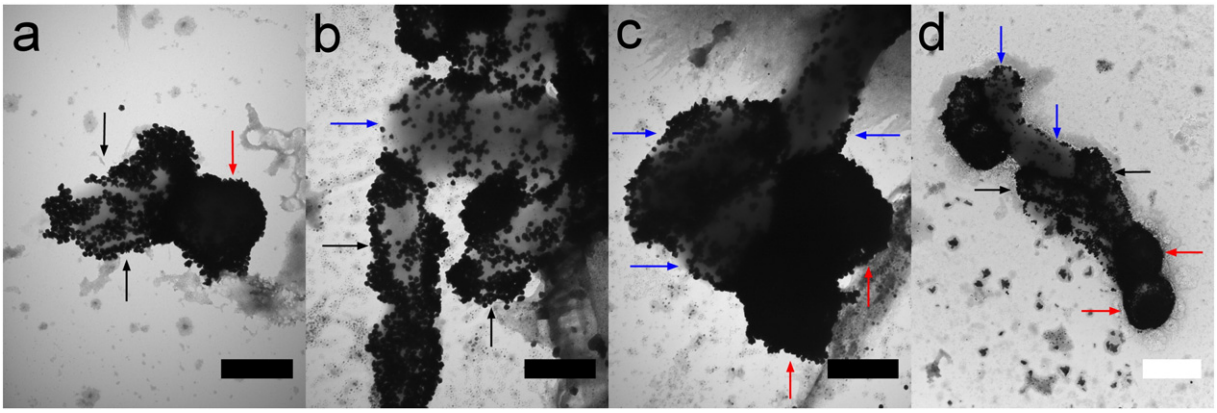

Fig. 3. TEM images of gold nanoparticles aggregating around bacteria mixtures: a) *Pseudomonas aeruginosa* (black arrows) + *Staphylococcus aureus* (red arrows), b) *P. aeruginosa* + *Escherichia coli* (blue arrows), c) *E. coli* + *S. aureus*, d) *P. aeruginosa* + *E. coli* + *S. aureus*, black scale bars are 500 nm, white scale bar is 1000 nm.

linear fit can be obtained for each sample, with the slope and intercept presented in Table 1. Quantitatively, it can be confirmed that saline sample shows almost no change with a slope of 0.000, while *P. aeruginosa* and *S. aureus* with slopes of 0.046 and 0.059 respectively show more changes compared to *E. coli* (slope of 0.007). The high R^2 values observed for all samples confirm good fit of the linear model in the first 2 min of data. A low R^2 value is obtained for the saline sample and is expected, because the response does not change over time, resulting in a slope of 0. Table 1 highlights that each sample is defined by a unique line, characterized by its slope and intercept. These values can be used for training the "chemical nose" and then for identifying which bacteria or mixture are present, as demonstrated previously [18,19]. Only 2 min of the spectral data were required for generating Fig. 2 using the portable spectrophotometer. Thus, if the "chemical nose" is coupled with this spectrophotometer design, polymicrobial infections can be rapidly diagnosed at the point-of-care.

3.2. TEM images of bacterial mixtures

We have previously demonstrated that the color change in gold nanoparticles is due to their aggregation around bacteria [17,18,28]. In order to study the nanoparticle aggregation in bacterial mixtures, these samples were imaged using transmission electron microscopy (TEM) and are presented in Fig. 3. The TEM images highlight that within the mixtures, each bacterial species maintains their affinity to nanoparticles. This allows us to identify which bacterium is being observed under the microscope. For example, *P. aeruginosa* shows a unique pattern of aggregation, where some areas are left bare and others show high aggregation, which is similar to that seen with *Stenotrophomonas maltophilia* in a previous study [18]. In comparison, *S. aureus* shows almost complete coverage due to the teichoic acids present on the surface. Thus, *P. aeruginosa* and *S. aureus* can be easily distinguished in Fig. 3a, not only by their size and shape but also due to their affinity for nanoparticles. Similarly, *E. coli* generally shows a lower but relatively uniform aggregation of nanoparticles on its cell walls. This is clear in Fig. 3b and c, where *P. aeruginosa* and *S. aureus* show more aggregation than *E. coli* respectively. Finally, Fig. 3d exemplifies all the qualities of the three bacteria observed together, where each bacterial species can still be distinguished. Thus, not only does the "chemical nose" serve as a platform for colorimetric detection, it can also be used as a tool for staining bacteria in a characteristic manner.

4. Discussion

We employed a CCD spectrophotometer to rapidly acquire absorption spectra [26]. Previously, similar designs have been extensively explored for portable detection with the help of smartphones and portable scanners [9,11,24]. Thus, the results demonstrated here can be easily translated for use in a smartphone accessory, which would allow for simple deployment at the point-of-care. Additionally, the use of PCA as a mathematical tool seems to overcome the considerable noise in the spectra, since the principal component 1 plot (Fig. 2) appears smoother than the raw data (Fig. 1). This analysis can be incorporated into a smartphone application in a manner similar to that used for label-free detection of proteins [9]. An easy-to-use interface will promote the deployment of the detection system in developing countries and in rural areas of developed countries, where access to equipment and trained personnel are limited [4,30].

The "chemical nose" produces a distinct degree and rate of color change for each of the bacterial samples because of the surface features of bacteria [15–18,21,28,31]. The cell walls of the bacteria contain unique compositions and orientations of lipids, proteins, and polysaccharides, which can interact with cationic gold nanoparticles [32–34]. In the case of Gram-positive bacteria such as *S. aureus*, most of the interactions are due to the polyanionic teichoic acids [35,36], while in the case of Gram-negative bacteria such as *E. coli* and *P. aeruginosa*, the interactions are governed by lipopolysaccharides [20,37]. Additionally, the extracellular polymeric matrix can play a role in preventing aggregation of the gold nanoparticles as may be the case for *E. coli* [19,38,39]. It has also been shown that lipids can exhibit specific domains within the cell walls upon addition of a cationic molecule [23] such as CTAB and this would explain the specific patterns of aggregation observed in the case of *P. aeruginosa*. Thus, a unique "smell" in the form of spectral response can be obtained for each sample in question for training the "chemical nose" and then an unknown spectrum can be matched with the training set, using techniques such as linear discriminant analysis to determine its identity.

5. Conclusions

A versatile "chemical nose" biosensor has been presented here that can diagnose monomicrobial and polymicrobial infections rapidly at the point-of-care. This was possible without complex modification of gold nanoparticles with biomolecules and by using a simple spectrophotometer design. The design can also be translated to a smartphone for widespread use in health, food, and environmental applications.

Supplementary data to this article can be found online at http://dx.doi.org/10.1016/j.sbsr.2016.05.004.

Acknowledgements

This work was financially supported by the Natural Sciences and Engineering Research Council of Canada (NSERC). M. S.V. is grateful for the NSERC Vanier Canada Graduate Scholarship and the Banting

Postdoctoral Fellowship. P. Z. C. and J.M.T. are thankful for the NSERC Undergraduate Student Research Award.

References

[1] C. Kaittanis, S. Santra, J.M. Perez, Emerging nanotechnology-based strategies for the identification of microbial pathogenesis, Adv. Drug Deliv. Rev. 62 (2010) 408–423.
[2] P. Tallury, A. Malhotra, L.M. Byrne, S. Santra, Nanobioimaging and sensing of infectious diseases, Adv. Drug Deliv. Rev. 62 (2010) 424–437.
[3] S.B. Shinde, C.B. Fernandes, V.B. Patravale, Recent trends in in-vitro nanodiagnostics for detection of pathogens, J. Control. Release 159 (2012) 164–180.
[4] A. Niemz, T.M. Ferguson, D.S. Boyle, Point-of-care nucleic acid testing for infectious diseases, Trends Biotechnol. 29 (2011) 240–250.
[5] M.S. Verma, J.L. Rogowski, L. Jones, F.X. Gu, Colorimetric biosensing of pathogens using gold nanoparticles, Biotechnol. Adv. (2015).
[6] V.K. Upadhyayula, Functionalized gold nanoparticle supported sensory mechanisms applied in detection of chemical and biological threat agents: a review, Anal. Chim. Acta 715 (2012) 1–18.
[7] K. Saha, S.S. Agasti, C. Kim, X. Li, V.M. Rotello, Gold nanoparticles in chemical and biological sensing, Chem. Rev. 112 (2012) 2739–2779.
[8] A.W. Martinez, S.T. Phillips, E. Carrilho, S.W. Thomas 3rd, H. Sindi, G.M. Whitesides, Simple telemedicine for developing regions: camera phones and paper-based microfluidic devices for real-time, off-site diagnosis, Anal. Chem. 80 (2008) 3699–3707.
[9] D. Gallegos, K.D. Long, H. Yu, P.P. Clark, Y. Lin, S. George, et al., Label-free biodetection using a smartphone, Lab Chip 13 (2013) 2124–2132.
[10] O. Mudanyali, S. Dimitrov, U. Sikora, S. Padmanabhan, I. Navruz, A. Ozcan, Integrated rapid-diagnostic-test reader platform on a cellphone, Lab Chip 12 (2012) 2678–2686.
[11] H. Zhu, U. Sikora, A. Ozcan, Quantum dot enabled detection of *Escherichia coli* using a cell-phone, Analyst 137 (2012) 2541–2544.
[12] H.M. Azzazy, M.M. Mansour, T.M. Samir, R. Franco, Gold nanoparticles in the clinical laboratory: principles of preparation and applications, Clin. Chem. Lab. Med. 50 (2012) 193–209.
[13] S.S. Agasti, S. Rana, M.H. Park, C.K. Kim, C.C. You, V.M. Rotello, Nanoparticles for detection and diagnosis, Adv. Drug Deliv. Rev. 62 (2010) 316–328.
[14] V. Rotello, Sniffing out cancer using “chemical nose” sensors, Cell Cycle 8 (2009) 3615–3616.
[15] U.H. Bunz, V.M. Rotello, Gold nanoparticle-fluorophore complexes: sensitive and discerning “noses” for biosystems sensing, Angew. Chem. Int. Ed. Eng. 49 (2010) 3268–3279.
[16] O.R. Miranda, X. Li, L. Garcia-Gonzalez, Z.J. Zhu, B. Yan, U.H. Bunz, et al., Colorimetric bacteria sensing using a supramolecular enzyme-nanoparticle biosensor, J. Am. Chem. Soc. 133 (2011) 9650–9653.
[17] M.S. Verma, P.Z. Chen, L. Jones, F.X. Gu, Branching and size of CTAB-coated gold nanostars control the colorimetric detection of bacteria, RSC Adv. 4 (2014) 10660–10668.
[18] M.S. Verma, P.Z. Chen, L. Jones, F.X. Gu, “Chemical nose” for the visual identification of emerging ocular pathogens using gold nanostars, Biosens. Bioelectron. 61 (2014) 386–390.
[19] M.S. Verma, S. Wei, J.L. Rogowski, J.M. Tsuji, P.Z. Chen, C. Lin, et al., Interactions between bacterial surface and nanoparticles govern the performance of “chemical nose” biosensors, Biosens. Bioelectron. 83 (2016) 115–125.
[20] J. Sun, J. Ge, W. Liu, X. Wang, Z. Fan, W. Zhao, et al., A facile assay for direct colorimetric visualization of lipopolysaccharides at low nanomolar level, Nano Res. 5 (2012) 486–493.
[21] S.C. Hayden, G. Zhao, K. Saha, R.L. Phillips, X. Li, O.R. Miranda, et al., Aggregation and interaction of cationic nanoparticles on bacterial surfaces, J. Am. Chem. Soc. 134 (2012) 6920–6923.
[22] K. Matsumoto, J. Kusaka, A. Nishibori, H. Hara, Lipid domains in bacterial membranes, Mol. Microbiol. 61 (2006) 1110–1117.
[23] R.M. Epand, R.F. Epand, Lipid domains in bacterial membranes and the action of antimicrobial agents, Biochim. Biophys. Acta 1788 (2009) 289–294.
[24] Z.J. Smith, K. Chu, A.R. Espenson, M. Rahimzadeh, A. Gryshuk, M. Molinaro, et al., Cell-phone-based platform for biomedical device development and education applications, PLoS ONE 6 (2011) e17150.
[25] J. Liu, Y. Lu, Preparation of aptamer-linked gold nanoparticle purple aggregates for colorimetric sensing of analytes, Nat. Protoc. 1 (2006) 246–252.
[26] J.H. Teichroeb, P.Z. McVeigh, J.A. Forrest, Influence of nanoparticle size on the pH-dependent structure of adsorbed proteins studied with quantitative localized surface plasmon spectroscopy, Eur. Phys. J. E. Soft Matter. 30 (2009) 157–164.
[27] W. Lu, A.K. Singh, S.A. Khan, D. Senapati, H. Yu, P.C. Ray, Gold nano-popcorn-based targeted diagnosis, nanotherapy treatment, and in situ monitoring of photothermal therapy response of prostate cancer cells using surface-enhanced Raman spectroscopy, J. Am. Chem. Soc. 132 (2010) 18103–18114.
[28] M.S. Verma, P.Z. Chen, L. Jones, F.X. Gu, Controlling “chemical nose” biosensor characteristics by modulating gold nanoparticle shape and concentration, Sensing and Bio-Sensing Research. 5 (2015) 13–18.
[29] J. Dantam, H. Zhu, F. Stapleton, Biocidal efficacy of silver-impregnated contact lens storage cases in vitro, Invest. Ophthalmol. Vis. Sci. 52 (2011) 51–57.
[30] D.A. Giljohann, C.A. Mirkin, Drivers of biodiagnostic development, Nature 462 (2009) 461–464.
[31] Y. Wan, Y. Sun, P. Qi, P. Wang, D. Zhang, Quaternized magnetic nanoparticles-fluorescent polymer system for detection and identification of bacteria, Biosens. Bioelectron. 55 (2014) 289–293.
[32] J.M. DiRienzo, K. Nakamura, M. Inouye, The outer membrane proteins of gram-negative bacteria: biosynthesis, assembly, and functions, Annu. Rev. Biochem. 47 (1978) 481–532.
[33] W.W. Navarre, O. Schneewind, Surface proteins of gram-positive bacteria and mechanisms of their targeting to the cell wall envelope, Microbiol. Mol. Biol. Rev. 63 (1999) 174–229.
[34] C.J. Boonaert, P.G. Rouxhet, Surface of lactic acid bacteria: relationships between chemical composition and physicochemical properties, Appl. Environ. Microbiol. 66 (2000) 2548–2554.
[35] V. Berry, A. Gole, S. Kundu, C.J. Murphy, R.F. Saraf, Deposition of CTAB-terminated nanorods on bacteria to form highly conducting hybrid systems, J. Am. Chem. Soc. 127 (2005) 17600–17601.
[36] V. Berry, R.F. Saraf, Self-assembly of nanoparticles on live bacterium: an avenue to fabricate electronic devices, Angew. Chem. Int. Ed. Eng. 44 (2005) 6668–6673.
[37] Y. Hong, D.G. Brown, Cell surface acid-base properties of *Escherichia coli* and *Bacillus brevis* and variation as a function of growth phase, nitrogen source and C:N ratio, Colloids Surf. B: Biointerfaces 50 (2006) 112–119.
[38] B. Vu, M. Chen, R.J. Crawford, E.P. Ivanova, Bacterial extracellular polysaccharides involved in biofilm formation, Molecules 14 (2009) 2535–2554.
[39] N. Joshi, B.T. Ngwenya, C.E. French, Enhanced resistance to nanoparticle toxicity is conferred by overproduction of extracellular polymeric substances, J. Hazard. Mater. 241-242 (2012) 363–370.